# Lithography-free, broadband, omnidirectional, and polarization-insensitive thin optical absorber

Fei Ding, Lei Mo, Jianfei Zhu, and Sailing He

Citation: Applied Physics Letters **106**, 061108 (2015); doi: 10.1063/1.4908182
View online: http://dx.doi.org/10.1063/1.4908182
View Table of Contents: http://scitation.aip.org/content/aip/journal/apl/106/6?ver=pdfcov
Published by the AIP Publishing



# Lithography-free, broadband, omnidirectional, and polarization-insensitive thin optical absorber

Fei Ding,[1,a)] Lei Mo,[1,a)] Jianfei Zhu,[1] and Sailing He[1,2,3,b)]
[1]*State Key Laboratory of Modern Optical Instrumentations, Centre for Optical and Electromagnetic Research, Zhejiang University, Hangzhou 310058, China*
[2]*ZJU-SCNU Joint Research Center of Photonics, Centre for Optical and Electromagnetic Research, South China Academy of Advanced Optoelectronics, South China Normal University (SCNU), Guangzhou 510006, China*
[3]*Department of Electromagnetic Engineering, School of Electrical Engineering, Royal Institute of Technology, S-100 44 Stockholm, Sweden*

(Received 17 December 2014; accepted 3 February 2015; published online 11 February 2015)

We have proposed and experimentally demonstrated a lithography-free, broadband, thin optical absorber composed of planar multilayered dielectric and metal films, which can cover the total visible wavelength range with simulated and experimental absorption efficiencies higher than 90%. Moreover, the absorption is insensitive to the polarization and angle of incidence. Such a planar device is much easier to fabricate compared with other broadband absorbers with complicated structures and may have potential applications in solar energy harvesting and controllable thermal emission. © *2015 AIP Publishing LLC*. [http://dx.doi.org/10.1063/1.4908182]

Thin-film optical perfect absorbers, which can completely absorb all incident light at specific frequencies without producing any reflection, transmission, or scattering within a few hundred nanometers, are increasingly appealing in many fields of science and technologies, e.g., sensing, controllable thermal emission, and solar energy harvesting.[1–4] However, such thin-film optical perfect absorbers are extremely difficult to construct as there do not exist many natural materials that could absorb light over a wide wavelength range and for a wide range of incident angles.

A possible method to realize efficient light absorption is to use various plasmonic structures, such as micro-cavities,[5] strips,[6,7] and subwavelength slits.[8,9] Metamaterials are also promising candidates for designing stable thin-film perfect absorbers, exhibiting wavelength scalability, thin thickness, and angle or polarization insensitivity.[10–12] However, the aforementioned absorbers often tend to be narrow banded owing to their resonant nature, which is inefficient for many practical applications such as solar energy harvesting. Blending various strong resonators operating at several neighboring frequencies together is a direct and effective way to increase the absorption bandwidth.[13–18] In addition to this, there have been other methods addressing this issue, such as adiabatic nanofocusing of gap surface plasmon modes excited by the scattering off subwavelength-sized wedges[19] and the excitation of slow-wave modes.[20–22]

However, in those broadband absorbers composed of nano-structures,[13–22] their fabrication involved electron beam lithography or focused ion beam milling, which are time-consuming, costly, and only suitable over small areas (usually less than 1 $mm^2$). Recently, lithography-free, wafer-scale metasurfaces have been proposed and designed for total absorption control.[23–26] To further improve the light absorption efficiency and simplify the fabrication process, here we propose a broadband optical perfect absorber consisting of continuous, optically thin silicon dioxide ($SiO_2$) and titanium (Ti) films on a gold (Au) coated substrate. The highly efficient broadband absorption is ascribed to the matched impedance and the large intrinsic absorption of Ti in the visible frequency. We experimentally demonstrate that this absorber can absorb 95% of visible light. Moreover, optical measurements show that the absorption performance is insensitive to the polarization of incident light, and high absorption persists when the incident angle is less than 40°.

The planar broadband optical absorber consists of two pairs of alternating thin $SiO_2$ and Ti films and a flat continuous Au film. The three-dimensional (3D) configuration and the cross-sectional view of the proposed structure are shown in Fig. 1(a). The thicknesses of the $SiO_2$ and Ti layers are $t_s = 80$ nm and $t_m = 12$ nm, respectively. The thickness of the bottom Au layer is $d = 150$ nm, which is large enough to block all light transmission.

For this planar symmetric structure, we use a two-dimensional (2D) model to simplify calculations, as shown in Fig. 1(a). In this 2D model, a plane wave of TM polarization (magnetic field is polarized along the $y$-axis) or TE polarization (electric field is polarized along the $y$-axis) impinges on the structure along the $z$-direction as an excitation source. Two different numerical methods are used to calculate the absorption spectra. The first method is the finite element method (FEM).[27] In the simulation, a periodic boundary condition is used in the $x$-direction. Since the structure is uniform along the $x$-axis, the period can be set arbitrarily (period is set to be 400 nm in our simulation). Meanwhile, an analytical method based on the transfer matrix is also used to calculate the reflection and transmission coefficients.[28] Here, all the materials are dispersive, and the corresponding permittivities within the visible range are taken from Ref. 29 ($SiO_2$ and Au) and Ref. 30 (Ti). The absorption is calculated from the scattering parameters as

a)F. Ding and L. Mo contributed equally to this work.
b)Author to whom correspondence should be addressed. Electronic mail: sailing@kth.se

 

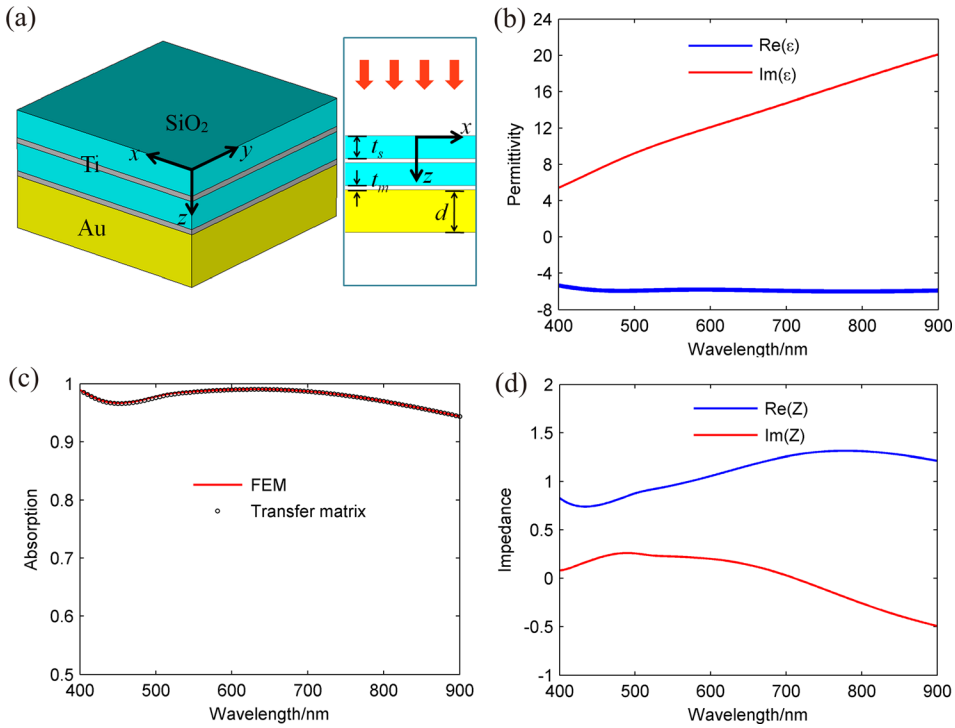


FIG. 1. Design of the planar optical absorber. (a) Schematic of the planar absorber. The cross-sectional view is shown with the denoted geometrical parameters. $t_s = 80\,\text{nm}$, $t_m = 12\,\text{nm}$, and $d = 150\,\text{nm}$. (b) Relative permittivity of Ti in visible frequency. (c) Simulated absorption spectrum under normal incidence (solid: FEM and symbol: transfer matrix). (d) Retrieved normalized impedance from the transfer matrix method.

$A(\lambda) = 1 - R(\lambda) - T(\lambda)$, where $R(\lambda)$ represents the reflection and $T(\lambda)$ represents the transmission, which is zero here. Fig. 1(c) shows the absorption spectra under normal incidence calculated by the FEM and the transfer matrix method represented by the solid line and the circle symbols, respectively. The results obtained by the two methods show negligible differences, which confirm that our numerical analysis here is reliable. Notably, one can see that over 94% of the incident light is dissipated within this planar absorber in a rather broad wavelength range from 400 nm to 900 nm, covering the total visible frequency range. The retrieved normalized effective impedance of this multilayered structure is plotted in Fig. 1(d). As can be observed, the impedance is approximately matched with that of the free space, eliminating the reflection. In addition, due to the high loss of Ti [Fig. 1 (b)], the incident wave can be absorbed in the thin Ti films and the bottom Au layer, resulting in wide band strong light absorption.

In the practical applications, such as photovoltaic solar-thermal power generation and blackbody thermal emitters, the absorption should be less sensitive to the incident angle ($\theta$). We performed FEM full-wave simulations to verify the angle dependence for both TM polarization (the magnetic field of the incident light is kept parallel to the y-axis) and TE polarization (the electric field of the incident light is kept parallel to the y-axis), as shown in Figure 2. In the simulation, $\theta$ varies from 0° to 80° in steps of 5°. Fig. 2 shows that the absorption effect is nearly robust for a relatively wide range of incident angles. For both polarizations, it can be seen that the ultra-broadband absorption response can be achieved when $\theta$ is below 40°, and the absorption still remains above 80% even when $\theta$ reaches 60°.

To experimentally observe the broadband absorption performance, we fabricated a multilayered planar absorber using a standard thin-film processing technology. The fabrication of the multilayered films started with a 150 nm Au film deposited on a flat silicon substrate using sputtering deposition at a deposition rate of 0.5 nm/s. The fabrication process was followed by depositing 2 pairs of thin, alternating Ti (12 nm)/$SiO_2$ (80 nm) layers onto the Au film using e-beam evaporation. The film growth rate for $SiO_2$ and Ti was 0.04 nm/s and 0.3 nm/s, respectively. In Fig. 3(a), we show a photograph of the fabricated sample (in the middle). For comparison, the images of the Au-coated silicon wafer

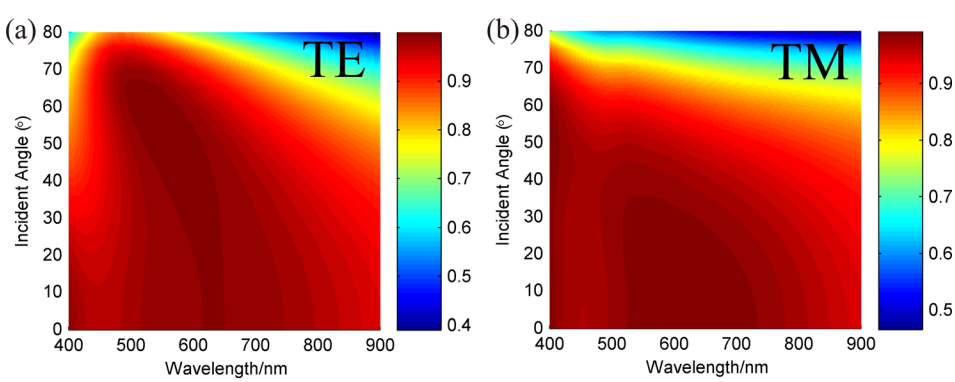


FIG. 2. Dependence of the absorption performance on the incident angle for the planar absorber for TE (a) and TM (b) polarizations.

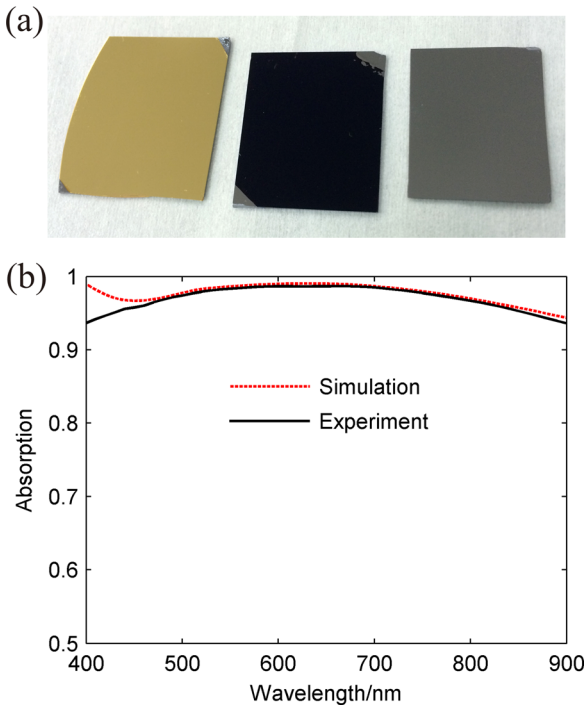


FIG. 3. Experimental result of the absorber. (a) Photograph of (from left to right) an Au-coated silicon wafer, fabricated sample, and silicon wafer. (b) Comparison between the experimental absorption (dashed line) and simulated absorption (solid line). The incident light is unpolarized and the incident angle is 8°.

and plain silicon wafer are also presented. From the photograph, one can easily tell that the middle sample exhibits a very high level of absorption across the visible spectral range.

Owing to the large-area, flat, and uniform surface of the fabricated sample, the reflection measurement is conducted by using a homemade integrating sphere to verify the calculated results. The incident light is unpolarized, and the minimum incident angle of this system is 8°. In such a reflection measurement, both the specular and diffusive signals are included in the reflection spectrum. The measured absorption spectrum of this multilayered structure is shown in Fig. 3(b). Impressively, the measured absorption is above 90% in the spectrum range from 400 nm to 900 nm. This planar sample exhibits a maximum absorption of 98.69%, and on average it can absorb 96.03% of the visible light. This explains why the sample appears to be black. Taking into account possible fabrication imperfections as well as measurement error, there is remarkably good agreement between the simulated and experimental results.

Moreover, the absorption spectra under oblique incidence for the unpolarized light are also measured with the same integrating sphere [Fig. 4(b)]. From Fig. 4(b), it is clearly seen that high absorption is experimentally persistent with varying incident angles. We also plot the calculated absorption for the unpolarized light at different incident angles, shown in Fig. 4(a). The corresponding simulated unpolarized absorbance curves are obtained by averaging the absorption spectra of the TE and TM polarizations at each incident angle. Overall, our multilayered planar absorber is insensitive to the changes in polarization and incident angles.

The bottom Au film plays a really important role in the absorption process. If it is removed, a part of the incident light will transmit through the absorber structure directly and the absorption effect will become weak [Fig. 5(a)]. Since Au is lossy, it can partially absorb the incident wave, especially at short wavelengths. To quantify the energy absorbed by different materials within this planar absorber, we integrated the simple equation of $P_{abs} = \frac{1}{2}\omega\varepsilon''|\vec{E}|^2$ over some material volume, where $\omega$ is the angular frequency, $\varepsilon$" is the imaginary part of the permittivity, and $E$ is the electric field amplitude. From Figs. 5(b) and 5(c), it is noted that the Ti layers dominate the total absorption in the whole investigated wavelength range, while the absorption in the Au substrate is weak. This indicates that the Au substrate mainly works as a reflection mirror and contributes little to the direct absorption of the incident light. In the short wavelength range where $\lambda < 550$ nm, the Au substrate can directly dissipate some of the incident energy, which is attributed to the intrinsically high loss of Au. Another interesting phenomenon is that most of the energy is absorbed (or most of the heat is generated) in the top Ti film (the absorption in the bottom Ti film is weak) within the working wavelength range, resulting from the highly lossy nature of Ti film. When light impinges on the structure, about half of the power is first dissipated within the top Ti film and the transmitted light which can reach the bottom Ti film is partially absorbed by the bottom Ti film or Au substrate. Then the remaining light is reflected by the Au substrate and bounces back and forth multiple times in this multilayered cavity, increasing the absorption in Ti films. That is why the absorption of the top Ti film is stronger. Besides the absorption that the bottom Ti film provides, it can also work as an adhesion layer between the gold substrate and $SiO_2$ layer.

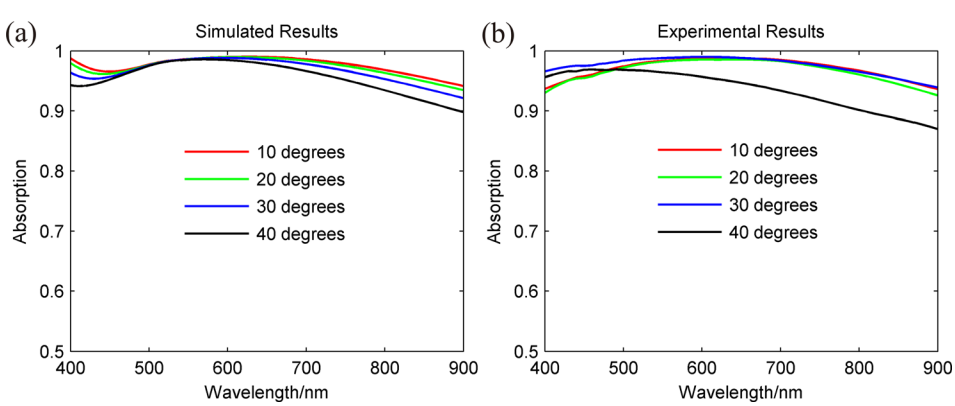


FIG. 4. (a) Simulated and (b) measured absorption for the unpolarized light at selected incident angles of 10°, 20°, 30°, and 40°.

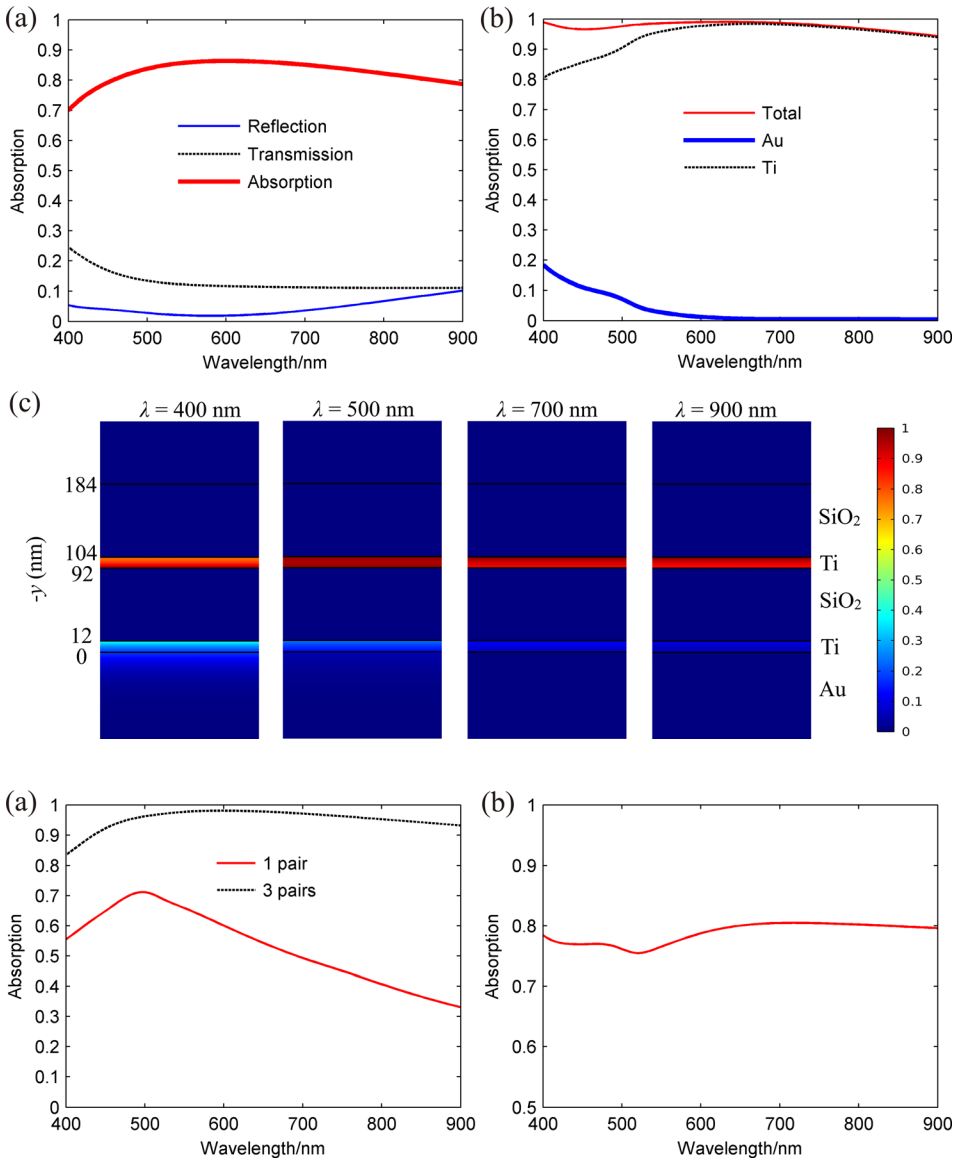


FIG. 5. Mechanism of broadband absorption. (a) Absorption, transmission, and reflection spectra for the modified planar absorber without the bottom Au layer. (b) Power absorbed at different materials within the absorber. (c) Resistive heat distribution for a normal incident of light at 400 nm, 500 nm, 700 nm, and 900 nm.

FIG. 6. Influence of some structure parameters on the absorption. (a) Absorption spectra for the structures composed of different number of $SiO_2$-Ti pairs. (b) Absorption spectra for the modified structure composed of 2 pairs of alternating Ti and $SiO_2$ films. The topmost layer is Ti film and the geometry parameters are the same as those of absorber in Fig. 1(a).

Further studies about the dependence of absorption on the number of $SiO_2$-Ti pairs are presented in Fig. 6(a), while the thicknesses of the $SiO_2$ layer, Ti layer, and bottom Au layer are kept the same ($t_s = 80$ nm, $t_m = 12$ nm, and $d = 150$ nm). Once the structure is composed of single $SiO_2$-Ti pair, the absorption becomes rather weak [red solid line in Fig. 6(a)]. If the structure is consisting of more $SiO_2$-Ti pairs, such as 3 pairs, broadband high absorption maintains. However, the thicker structure will increase fabrication cost. Additionally, the order of the films (e.g., ended with $SiO_2$ or Ti) really impact the absorption performance. From Fig. 6(b), it is clearly seen that the absorption efficiency is lower than 81% if the topmost layer is Ti film compared with that of the absorber in Fig. 1(a).

In conclusion, we have realized a lithography-free, ultra-broadband thin optical absorber based on planar multilayered dielectric and metal films, which ensures high-efficiency, omni-directional, and polarization-insensitive light absorption covering the whole visible light range in both simulation and experiment. Impressively, the measured absorption is above 90% in the spectrum range from 400 nm to 900 nm, reaching an average of 96.03%. Specially, the fabrication of this structure is very simple, and it can be easily obtained over large areas (wafer scale) with standard thin-film deposition technology. These types of planar absorbers are promising candidates for improving the performance of thermo-photovoltaic systems. Moreover, because of the intrinsic planar configuration, our structure is highly scalable in fabrication and can be integrated and implemented in both micro- and macro-applications.

The authors acknowledge the support by the National Natural Science Foundation of China (Nos. 91233208, 61271016, and 61178062), the National High Technology Research and Development Program (863 Program) of China (No. 2012AA030402), a Guangdong Innovative Research Team Program (Grant No. 201001D0104799318), and Swedish VR grant (No. 621-2011-4620).

[1]C. M. Watts, X. Liu, and W. J. Padilla, Adv. Mater. **24**, OP98 (2012).
[2]Y. Cui, Y. He, Y. Jin, F. Ding, L. Yang, Y. Ye, S. Zhong, Y. Lin, and S. He, Laser Photonics Rev. **8**, 495 (2014).
[3]D. Kraemer, B. Poudel, H. P. Feng, J. C. Cavlor, B. Yu, X. Yan, Y. Ma, X. W. Wang, D. Z. Wang, A. Muto, K. McEnaney, M. Chiesa, Z. F. Ren, and G. Chen, Nat. Mater. **10**, 532 (2011).
[4]E. Rephaeli and S. H. Fan, Opt. Express **17**, 15145 (2009).

[5]T. V. Teperik, F. J. Garcia de Abajo, A. G. Borisov, M. Abdelsalam, P. N. Bartlett, Y. Sugawara, and J. J. Baumberg, Nat. Photonics **2**, 299 (2008).
[6]N. Bonod, G. Tayeb, D. Maystre, S. Enoch, and E. Popov, Opt. Express **16**, 15431 (2008).
[7]A. P. Hibbins, W. A. Murray, J. Tyler, S. Wedge, W. L. Barnes, and J. R. Sambles, Phys. Rev. B **74**, 073408 (2006).
[8]J. Le Perchec, P. Quemerais, A. Barbara, and T. Lopez-Rios, Phys. Rev. Lett. **100**, 066408 (2008).
[9]J. S. White, G. Veronis, Z. Yu, E. S. Barnard, A. Chandran, S. Fan, and M. L. Brongersma, Opt. Lett. **34**, 686 (2009).
[10]N. I. Landy, S. Sajuyigbe, J. J. Mock, D. R. Smith, and W. J. Padilla, Phys. Rev. Lett. **100**, 207402 (2008).
[11]X. L. Liu, T. Starr, A. F. Starr, and W. J. Padilla, Phys. Rev. Lett. **104**, 207403 (2010).
[12]N. Liu, M. Mesch, T. Weiss, M. Hentschel, and H. Giessen, Nano Lett. **10**, 2342 (2010).
[13]Y. Q. Ye, Y. Jin, and S. He, J. Opt. Soc. Am. B **27**, 498 (2010).
[14]K. Aydin, V. E. Ferry, R. M. Briggs, and H. A. Atwater, Nat. Commun. **2**, 517 (2011).
[15]Y. Cui, J. Xu, K. H. Fung, Y. Jin, A. Kumar, S. He, and N. X. Fang, Appl. Phys. Lett. **99**, 253101 (2011).
[16]L. Huang, D. R. Chowdhury, S. Ramani, M. T. Reiten, S. N. Luo, A. J. Taylor, and H. T. Chen, Opt. Lett. **37**, 154 (2012).
[17]M. G. Nielsen, A. Pors, O. Albrektsen, and S. I. Bozhevolnyi, Opt. Express **20**, 13311 (2012).
[18]J. Zhu, Z. Ma, W. Sun, F. Ding, Q. He, L. Zhou, and Y. Ma, Appl. Phys. Lett. **105**, 021102 (2014).
[19]T. Søndergaard, S. M. Novikov, T. Holmgaard, R. L. Eriksen, J. Beermann, Z. Han, K. Pedersen, and S. I. Bozhevolnyi, Nat. Commun. **3**, 969 (2012).
[20]Y. Cui, K. H. Fung, J. Xu, H. Ma, Y. Jin, S. He, and N. X. Fang, Nano Lett. **12**, 1443 (2012).
[21]F. Ding, Y. Cui, X. Ge, Y. Jin, and S. He, Appl. Phys. Lett. **100**, 103506 (2012).
[22]F. Ding, Y. Jin, B. Li, H. Cheng, L. Mo, and S. He, Laser Photonics Rev. **8**(6), 946–953 (2014).
[23]V. G. Kravets, S. Neubeck, and A. N. Grigorenko, Phys. Rev. B **81**, 165401 (2010).
[24]M. K. Hedayati, M. Javaherirahim, B. Mozooni, R. Abdelaziz, A. Tavassolizadeh, V. S. Kiran Chakravadhanula, V. Zaporojtchenko, T. Strunkus, F. Faupel, and M. Elbahri, Adv. Mater. **23**, 5410 (2011).
[25]M. A. Kats, D. Sharma, J. Lin, P. Genevet, R. Blanchard, Z. Yang, M. M. Qazilbash, D. N. Basov, S. Ramanathan, and F. Capasso, Appl. Phys. Lett. **101**, 221101 (2012).
[26]D. Wang, W. Zhu, M. D. Best, J. P. Camden, and K. B. Crozier, Sci. Rep. **3**, 2867 (2013).
[27]J. P. A. Bastos and N. Sadowski, *Electromagnetic Modeling by Finite Element Methods* (Marcel Dekker, New York, 2003).
[28]P. Yeh, *Optical Waves in Layered Media* (John Wiley & Sons, New York, 1988).
[29]E. D. Palik, *Handbook of Optical Constants of Solids* (Academic Press, New York, 1998).
[30]A. D. Rakić, A. B. Djurišić, J. M. Elazar, and M. L. Majewski, Appl. Opt. **37**, 5271 (1998).